

Evaluation of *Pseudomonas aeruginosa* Deacetylase LpxC Inhibitory Activity of Dual PDE4–TNF α Inhibitors: A Multiscreening Approach

Rameshwar U. Kadam, Divita Garg, Archana Chavan, and Nilanjan Roy*

Centre of Pharmacoinformatics, National Institute of Pharmaceutical Education and Research, Sector 67,
S.A.S Nagar-160 062, Punjab, India

Received August 18, 2006

In this study, we have focused on the implication of a multiscreening approach in the evaluation of *Pseudomonas aeruginosa* deacetylase LpxC inhibitory activity of dual PDE4–TNF α inhibitors. A genetic function approximation (GFA) directed quantitative structure–activity relationship (QSAR) model was developed for LpxC inhibition on the basis of reported biological activity (Kline and Andersen, *J. Med. Chem.* **2002**, *45*, 3112–3129). Subsequently, reported PDE4–TNF α inhibitors (Klienman and Campbell, *J. Med. Chem.* **1998**, *41*, 266–270) were screened using the QSAR model. Whereby, the compounds were predicted to have equipotent activity with the most potent compound in reported LpxC inhibitor series. A docking analysis of these compounds carried out on the LpxC homology model corroborated the initial results. The compounds were then validated using surface electronic properties analysis and subjected to an adsorption, distribution, metabolism, excretion, and toxicity filter. Taken together, a multiscreening strategy was used to validate potential leads for LpxC inhibition.

INTRODUCTION

The major limiting factor in the implementation of virtual screening methods is that the methods that are efficient are not effective (like similarity searching and various ligand-based approaches), and those that are effective are not efficient (like very accurate flexible docking and scoring analysis). Thus, in view of the above, a multilayer virtual screening protocol comprised of a screening layer, a prediction layer, and a validation layer has been envisaged.^{1–3} This multilayered screening approach integrates several virtual screening techniques in a systematic order according to their computational cost. The first layer is a preliminary *screening layer* that can evaluate a large number of compounds at minimal computational cost. For this part of the calculation, accurate numerical predictions of activity are not essential, but this layer may be used to exclude the compounds that are likely to be poor binders. Common feature pharmacophore- and fingerprint-based similarity searching are some of the methods that can be used in this layer. Either these methods can be used as a stand-alone wherein the choice of the method depends on the availability of structural and molecular data or a consensus of these models may be used. The prediction layer is the second layer which consists of approaches like hologram quantitative structure–activity relationships, binary descriptor-based quantitative structure–activity relationships (QSAR), comparative molecular field analysis, and so forth for in silico estimation of the biological activity. The molecules screened out by these two levels are then validated in the third layer, that is, the validation layer, which involves a structure-based binding energy predictor, which serves as a validation of the activity prediction.

The aim of this study was to evaluate the PDE4–TNF α dual inhibitors proposed as the metalloenzyme target inhibi-

tors⁴ for *Pseudomonas aeruginosa* deacetylase LpxC inhibitory activity using the multiscreening approach. Accordingly, a QSAR model was developed, which was used to preliminarily screen PDE4–TNF α inhibitors⁵ to obtain possible leads for *P. aeruginosa* deacetylase LpxC inhibition. The compounds were then meticulously validated using a ternary filter consisting of docking, surface electronic properties analysis, and finally adsorption, distribution, metabolism, excretion, and toxicity (ADME/T) analysis.

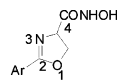
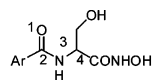
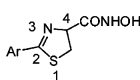
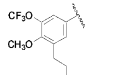
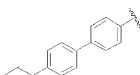
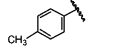
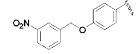
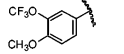
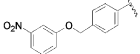
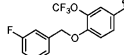
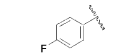
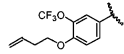
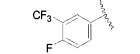
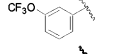
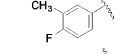
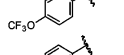
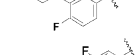
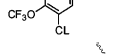
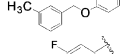
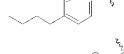
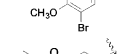
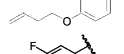
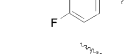
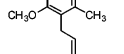
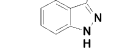
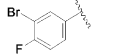
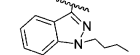
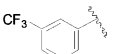
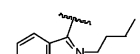
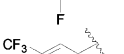
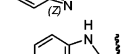

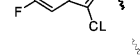
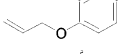
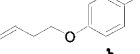
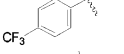
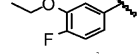
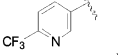
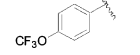
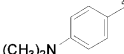
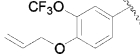
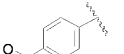
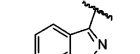
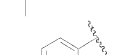
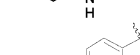
MATERIALS AND METHODS

Data Set. In this study, the LpxC inhibitors reported by Kline et al.⁶ were used as a reference for the development of in silico models which were then used to evaluate the reported dual PDE4–TNF α inhibitors.⁵ As reported by Kline et al., the orientation at the 4 position in the ring is known to be of special importance; the compounds were removed if they were described as a racemic mixture or if their stereochemistry at the 4 position was not specified and the exact IC₅₀ not known.⁶ On this basis, the data set of 41 out of the 64 reported LpxC inhibitors was selected for QSAR analysis. The structures and experimental values of activity for the compounds used in this study are shown in Table 1.

The ligands under study were built using the SYBYL7.1 molecular modeling package installed on a Silicon Graphics Fuel workstation running on the IRIX 6.5 operating system.⁷ Since the crystal structure of the LpxC is not known, the basic skeleton and conformation for the most active molecule (i.e., **L3**) from the series was modeled and minimized using the PM3 Hamiltonian using MOPAC interfaced with SYBYL7.1. In order to generate accurate charge information, a single-point energy calculation was also performed using the AM1 Hamiltonian⁸ on the PM3 geometry. The rest of the molecules were built by changing the required substitution using **L3** as the template and were minimized similarly. Mulliken charges were assigned to all of the molecules.⁹

* Corresponding author phone: +91 172 2214682; fax: +91 172 2214692; e-mail: nilanjanroy@niper.ac.in.

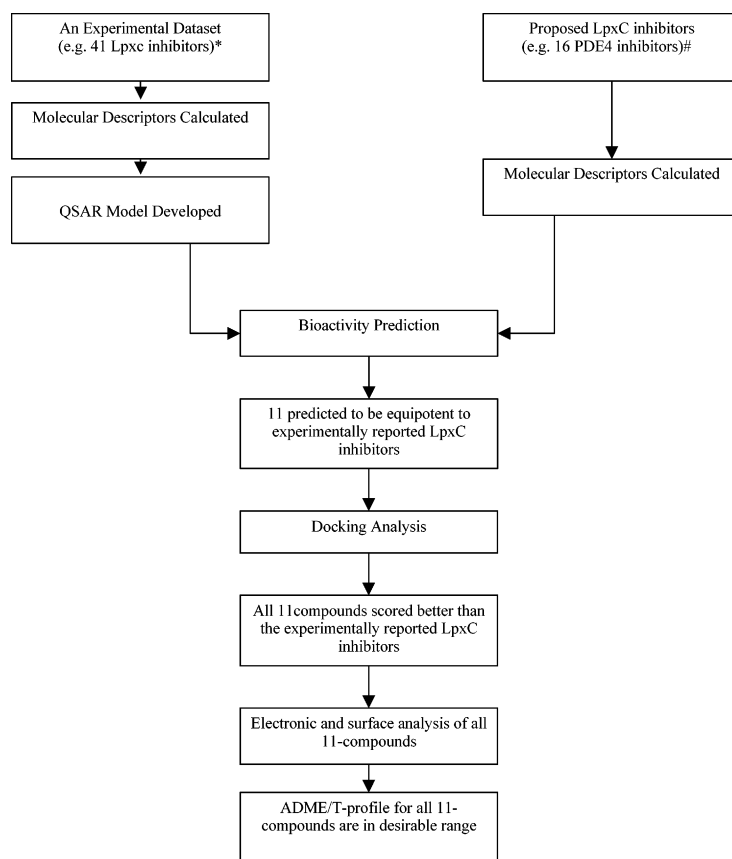
Table 1. Structures and Activities of 2-Aryloxazolines, Arylserines (A), 2-Arylthiazolines (B)^a

											
Mol ID	Ar	PIC ₅₀ (M)		Mol ID	Ar	PIC ₅₀ (M)		Mol ID	Ar	PIC ₅₀ (M)	
		Expt.	Predicted			Expt.	Predicted				
L1		6.30	6.75	L12		6.55	6.52				
L2		4.69	4.84	L13		6.00	6.30				
L3		6.79	6.48	L14*		6.25	6.07				
L4*		6.60	6.54	L15		5.22	5.08				
L5		6.45	6.20	L16		5.88	5.21				
L6		5.22	5.52	L17		5.92	5.16				
L7		5.30	5.39	L18*		6.02	5.74				
L8		4.52	5.16	L19		6.07	6.21				
L9		5.13	5.42	L20		5.04	5.71				
L10		5.25	5.11	L21*		5.48	4.98				
L11		6.00	5.71	L22		5.25	5.49				
L23		5.30	5.02	L33		5.00	4.96				
L24		4.60	4.99	L34*		4.92	4.74				
L25		5.60	5.11	L35*		5.80	5.84				
L26		5.65	5.73	L36 _A		5.40	5.20				
L27		5.10	5.14	L37		4.33	4.73				
L28		5.00	4.65	L38		5.81	5.50				
L29		5.30	5.56	L39 _A		5.12	6.20				
L30		4.74	4.96	L40* _A		4.89	5.30				
L31B		4.41	4.43	L41B		4.23	4.90				
L32		4.74	4.36	L42 [#]		>30(IC ₅₀ , μ M)					

^a “*” indicates test set compounds, and the remaining are training set compounds. “A” indicates aroylserines series, and “B” indicates 2-arylthiazolines series, and the remaining are 2-aryloxazolines series. “#” indicates that compound L42 was not used in any in silico studies reported herein.

Multiscreening Methodology. Our strategy mainly focused on the implication of a multilayer approach involving the use of a validated QSAR model developed from the

available series of reported LpxC inhibitors as a preliminary screening layer and the use of docking along with surface electronic properties analysis and ADME/T filter as a



* Kline and Andersen, *J. Med. Chem.* **2002**, 45, 3112-3129

Klienman and Campbell, *J. Med. Chem.* **1998**, 41, 266-270

Figure 1. Flow chart of multilayer approach involving integrated use of a descriptors-based QSAR model as preliminary screening layer, docking, MEPS, and ADME/T-based validation layer.

Table 2. Correlation Matrix of Molecular Descriptors Used in QSAR Model Development

Sr. No		Mor26P	Mor14V	Mor24U	H2U	HATS2P	PIC ₅₀
1	Mor26P	1.000					
2	Mor14v	0.306	1.000				
3	Mor24U	-0.076	0.328	1.000			
4	H2U	-0.148	0.346	0.385	1.000		
5	HATS2P	0.225	-0.093	0.175	-0.499	1.000	
6	PIC ₅₀	-0.458	-0.462	0.007	0.354	-0.383	1.000

validation layer. The general flow chart of the screening procedure is shown in (Figure 1) and includes the following major steps: (1) the development of a validated QSAR model using 3D descriptors for a data set of LpxC inhibitors with known structures and activities, (2) the calculation of molecular descriptors and prediction of biological activity for the PDE4-TNF α dual inhibitors proposed to be active LpxC inhibitors, (3) the selection of structures predicted to be equipotent ($4.58 \leq \text{PIC}_{50\text{pred}} \leq 5.48$) to the reported LpxC series, (4) the validation of selected structures by docking into a developed homology model of LpxC, (5) further confirmation using surface electronic properties analysis, and (6) final screening through ADME/T filters for the identification of druglike molecules among the screened hits.

QSAR Model Development and Activity Prediction. The data set of 41 molecules was divided into a training set containing 34 molecules and a test set containing 7 molecules so as to maintain structural and activity diversity in both of the sets. The molecular descriptors were calculated using DRAGON 5.0 software.¹⁰ A correlation matrix of the descriptors was prepared, and highly correlated descriptors

with a correlation value above 0.7 were removed from the study (Table 2). The remaining descriptors were used for genetic function approximation (GFA)¹¹⁻¹⁸ directed QSAR model development in the Cerius²4.10 software package.¹⁹

Docking Study. A homology model for *P. aeruginosa* deacetylase LpxC was used for the docking study of the molecules selected from the QSAR analysis. Docking experiments were carried out in the FlexX module in SYBYL7.1, which utilizes the incremental construction algorithm. The active site for the docking calculation was defined using the Site ID module in SYBYL7.1 on the *P. aeruginosa* deacetylase LpxC structure by retaining all residues which occurred in the radius of 6 Å from the pocket identified by site ID. The residues occurring in the active site and the hydrophobic nature of the site have been well-reported in the literature.²⁰⁻²¹ This was used as a criterion for the selection of the pocket from multiple pockets identified by Site ID (Figure 2 of the Supporting Information-2 file).

Surface Electronic Properties-Based Validation. The structures selected by docking and scoring analysis were

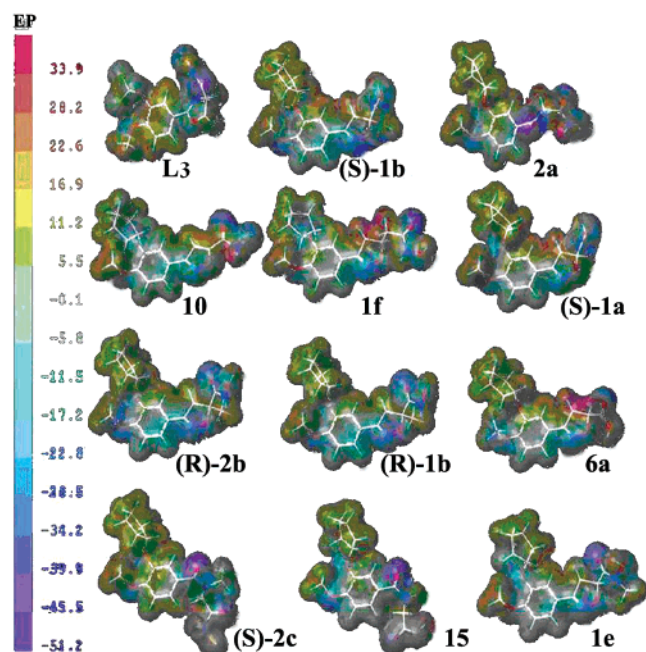


Figure 2. Molecular electrostatic potential (MEPS) surfaces property of the dual PDE4-TNF α inhibitors proposed as LpxC inhibitors compared with the known inhibitors of the LpxC (i.e., L3) on the same MEPS scale. Compound I indicates most active compound in LpxC inhibitors series (i.e., L3). Compounds (S)-1b to -1e indicate molecules proposed as LpxC inhibitors. The color ramp for EP ranges from red (most positive; 63.8 kcal/mol) to purple (most negative; -68.1 kcal/mol)

further validated by surface electronic properties analysis, that is, molecular electrostatic potential surface (MEPS) analysis. All MEPS calculations and visualization were carried out using the MOLCAD program implemented in the SYBYL7.1 molecular modeling package. MEP surfaces were generated and visualized (Figure 2).

ADME/T Prediction. To select only those molecules from the screened hits which possessed druglikeness and were potentially low on toxicity, that is, possessed a better chance of being successfully taken up as drug leads, ADME/T analysis was carried out. ADME/T studies were performed in Cerius²4.10. The molecules which were proven to be potentially druglike were ultimately considered as potential lead molecules.

RESULTS AND DISCUSSION

We developed a statistically significant model (eq 1) to predict pIC₅₀ for the data set which is shown in Table 1.

$$\begin{aligned} \text{Log}(1/\text{IC}_{50}) = & 5.155\,65 - 1.596\,14\text{mor14v} - 0.9239 < \\ & 2.485 - \text{H2U} > + 1.7411 < \text{mor24U} - 0.104 > - \\ & 3.1202 < \text{mor24U} - 0.505 > + 81.1483 < 0.101 - \\ & \text{HATS2p} > - 5.09371 < \text{mor26p} + 0.157 > \quad (1) \end{aligned}$$

$$\begin{aligned} N = 34, \text{LOF} = 0.347, r^2 = 0.813, r^2_{\text{adj}} = \\ 0.771, \text{F-test} = 17.515, \text{LSE} = 0.087, q^2 = \\ 0.732, \text{Bsr}^2 = 0.813, \text{Bsr}^2_{\text{error}} = 0.004, r^2_{\text{pred}} = 0.857 \end{aligned}$$

where N is number of compounds in the training set, LOF is the lack of fit, r^2 is the squared correlation coefficient, r^2_{adj} is the square of the adjusted correlation coefficient, F-test is a variance-related statistic that compares two models

differing by one or more variable to see if the more complex model is more reliable than the less complex one, the model is supposed to be good if the F-test is above a threshold value, LSE is the least-square error, q^2 is the square of the correlation coefficient of the cross-validation, r^2_{pred} is the predicted correlation coefficient calculated from the predicted activity of the test set compound. The model has good predictability, which is confirmed by the close r^2 and q^2 values. The fits of the QSAR model to the training set and test set are shown in Figure 3. The detailed descriptions of the variable used in the QSAR model and training and test set residual values are described in Tables 1–3 of the Supporting Information-1 file.

To be useful, a QSAR model must be predictive so that it can provide estimates of the activity of untested compounds similar to those in the data set used to construct the model. To determine the model's reliability and significance, both randomization and a full cross-validation procedure were performed for QSAR models developed for LpxC inhibitors. The randomization was done by repeatedly permuting the dependent variable set (i.e., the mean activity data). If the score of the original QSAR models proved better than those from the permuted data set, the model would be considered statistically significant. The results of the randomization test are presented in Table 4 of the Supporting Information-1 file. The regression coefficient, r , for the nonrandom QSAR model was 0.757, significantly better than those obtained from randomization data (mean $r = 0.377$, standard deviation = 0.113). Hence, the original GFA model could be considered to be significant.

Standard cross-validation in GFA encompasses the optimization of regression coefficients; it does not encompass the optimization of the choice of descriptors. That is, the regression model is validated only for the specific subset of descriptors obtained from GFA. In contrast, full cross-validation encompasses the entire algorithm, including the choice of descriptors and the optimization of regression coefficients. Each full cross-validation step finds the subset of descriptors for a training set of $N - 1$ compounds. The results based on the rules of "leave-one-out", "leave-two-out", "leave-five-out", "leave-seven-out", and "leave-nine-out" are shown in Table 5 of the Supporting Information-1 file. In other words, at each step, one, two, five, seven, or nine of 34 compounds were left out in the GFA training process. The process was repeated until every compound had been left out and predicted once. q^2 was then calculated on the remaining compounds in the data set. The GFA models proved to be very predictive, with good full q^2 values obtained when seven molecule were left out at a time. The narrow range of q^2 is indicative of the good predictability of the derived model.

This model is weighted with the atomic polarizability and radius of van der Waals which have a negative contribution to the log IC₅₀ value, leading to a decrease in affinity of the inhibitors for the binding site. The negative contribution of Morse descriptors (mor14v, mor24U, and mor26p) suggests how the interatomic distance corresponding to the addition of polar bulky substituents (e.g., -CH₃O) at different positions in the phenyl ring have their impact on activity (Table 1; Supporting Information-1, Table 3).

This QSAR model was then used to predict the activity values for the reported PDE4-TNF α inhibitors proposed to

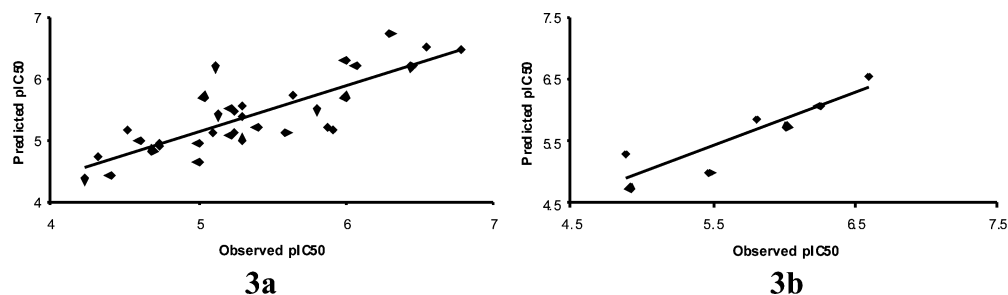
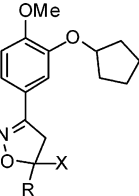
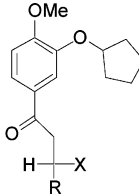
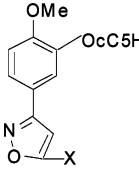


Figure 3. (a) Scatter plots of actual versus predicted activity for training set molecules (■). (b) Scatter plots of actual versus predicted activity for test set molecules (■).

Table 3. Dual PDE4–TNF α Inhibitors with Their Structure and Predicted Activity with QSAR Model Developed for LpxC Inhibitors

  			
1a-f, (R)-1a,b, (S)-1a,b, 5g, 6a 2a, (R)-2b,c, (S)-2b,c, 15 10			
compound	R	X	pIC ₅₀
(R)-1a	H	CONHOH	3.32
(R)-2c	i-Pr	CONHOH	3.86
(R)-1b	Me	CONHOH	4.58
(S)-1b	Me	CONHOH	4.64
1f	H	CH ₂ CONHOH	4.69
6a	H	CO ₂ H	4.79
(S)-1a	H	CONHOH	4.79
2a	H	CONHOH	4.83
5g	H	CONH ₂	4.86
(S)-2b	Me	CONHOH	5.05
(R)-2b	Me	CONHOH	5.05
1d	Pr	CONHOH	5.18
15	H	CO ₂ H	5.37
1e	H	CONMeOH	5.37
10			5.44

be active against LpxC deacetylase. The results of the predictions are shown in Table 3. The most potent molecule of the series used for model development was predicted at 6.48, and the minimum prediction was at 4.36. This was employed as the cutoff range for the selection of compounds from the PDE4–TNF α inhibitors under testing, resulting in the identification of 11 compounds.

In order to understand the docking mode of LpxC inhibitors and evaluate the LpxC inhibitory propensity of the proposed inhibitors, docking studies on a developed homology model were carried out (a detailed study about coordination geometry around the metal ion and optimization of the homology model are shown in Figure 1 and Table 1 of the Supporting Information-3 file). The template used for homology modeling (*Aquifex aeolicus* LpxC) is a cocrystal with Tu-514 (PDB ID: 1XXE). Thus, to validate the docking protocol, TU-514 was extracted from the crystal structure of LpxC and docked into the *P. aeruginosa* LpxC homology model. The docked TU-514 showed essentially the same conformation as the bound ligand with a root-mean-square value of 0.892 Å calculated using the FIT ATOM method in SYBYL 7.1.

Once the docking methodology was confirmed, the same protocol was used for the reported inhibitor of LpxC, that

is, **L3**, and the dual PDE4–TNF α inhibitors proposed as LpxC inhibitors. The binding pocket of LpxC inhibitors is formed by amino acids Met62, Ser63, Glu77, His78, Thr190, Phe191, Gly192, His237, Lys238, Asp241, Gly263, His264, and Ala265. Most of the amino acids are common to the binding pocket of the dual PDE4–TNF α inhibitors proposed as LpxC inhibitors. The binding modes of these predicted compounds are depicted in Figure 4. The binding mode of the most potent compound (**L3**) is shown for comparison. The docked conformation of **L3** essentially adopted a butterfly-like conformation within the LpxC binding pocket (Figure 4; **L3**). Moreover, in accordance with the reported experimental studies for LpxC substrate/inhibitors, the docked ligands could adopt a collection of alternative positions that were anchored by the hydroxamic acid group but left the phenyl ring free to pivot inside the hydrophobic pocket.²⁰ The carbonyl oxygen and nitrogen group of docked conformation of **L3** in *P. aeruginosa* LpxC essentially show H-bonding interactions with Asp241, His78, and Thr190 via Zn²⁺ (Table 4). Whereas, His 78, Thr190, and Lys238 act as side-chain donors which interact with the carbonyl oxygen of hydroxamic acid, the nitrogen of the oxazoline ring, and the oxygen of the phenyl ring, respectively. Whereas, Glu77 acts as side-chain acceptor (Figure 4; **L3**). The phenyl moiety made π -stacking interactions against the Phe191.

As compared to the most potent compound in the LpxC inhibitory series, these predicted compounds showed additional contacts with Met62 and Ser63, which explains the lower energy calculated by FlexX for predicted compounds as compared to **L3**. The presence of the *m*-pentoxy moiety and methoxy groups on the phenyl ring are chief determinants of the putative activity of these inhibitors. Compounds **2a** and **15** presented additional interactions between the hydroxamic acid and the amino acids Ser63 and Met61 (Figure 4). However, contacts with Phe191 were not observed for these two compounds. For the compounds (S)-**2c**, (R)-**2b**, and **15**, which lack the oxazoline ring structure at the 4 position of the hydroxamic acid moiety, a rotated conformation was predicted as compared to the butterfly-shaped orientation of the former nine dual PDE4–TNF- α inhibitors proposed as LpxC inhibitors (Figure 4). Almost all of these molecules showed π -stacking interactions with Phe191. The details of a docking analysis of 11 compounds are depicted in Table 4.

However, the docking results were not in accordance with the QSAR results; all of these compounds docked with a better score as compared to that of **L3** (Table 3). This is mainly due to the slightly different mode of binding of these inhibitors and the presence of a more positive potential moiety (pentoxy moiety) near the phenyl ring, which is

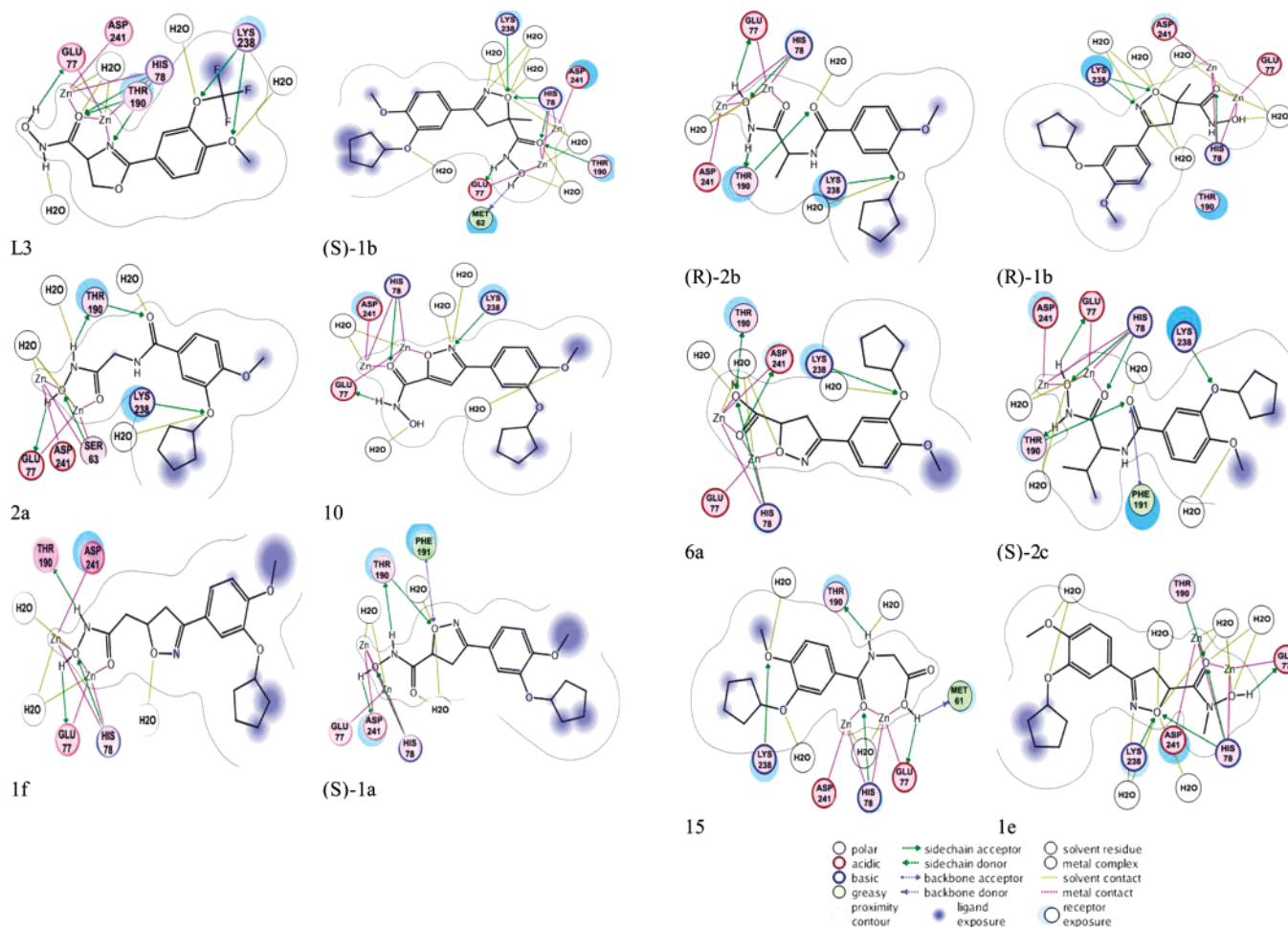


Figure 4. Docking of **L3** and proposed dual PDE4–TNF α inhibitors as LpxC inhibitors into LpxC binding pocket.

Table 4. Scores and Interactions of LpxC 20 and Proposed Dual PDE4–TNF α Inhibitors as LpxC Inhibitors

compound	score	interactions					
		H-bond	residues involved	π -stacking	residues involved	hydrophobic	residues involved
L3	–21.19	6	Lys238, His78, Thr190, Glu77	1	Phe 191	3	Met62, Gly192, Gly263
(S)-1b	–24.21	5	Lys238, His78, Thr190, Glu77	1	Phe 191	2	Met62, Gly192
2a	–28.66	5	Lys238, Ser63, Thr190, Glu77	1	Phe 191	3	Met62, Gly192, Gly263
10	–30.01	3	Lys238, His78, Glu77			2	Met62, Gly192
1f	–22.10	3	His78, Thr190, Glu77	1	Phe 191	2	Met62, Gly192
(S)-1a	–27.21	4	His78, Thr190, Asp241	1	Phe 191	2	Met62, Gly192
(R)-2b	–27.19	5	Lys238, His78, Thr190, Glu77	1	Phe 191	3	Met62, Gly192, Ala265
(R)-1b	–24.22	3	Lys238, His78,			4	Met62, Gly192, Gly263, Ala265
6a	–28.92	4	Lys238, His78, Thr190, Asp241	1	Phe 191	2	Met62, Gly192
(S)-2c	–25.29	5	Lys238, His78, Thr190, Glu77	1	Phe 191	2	Met62, Gly192
15	–25.19	4	Lys238, His78, Thr190, Glu77	1	Phe 191	4	Met62, Gly192, Gly263, Ala265
1e	–32.65	4	Lys238, His78, Thr190, Glu77			2	Met62, Gly192

the chief determinant for burying into the hydrophobic pocket in the active site of LpxC.

So, to corroborate the analysis of structural requirements of LpxC inhibitors with the activity, a detailed surface electronic properties analysis was performed on the dual PDE4–TNF α inhibitors proposed as LpxC inhibitors and **L3** on the basis of MEPS. MEP is a popular indicator of electrophilic and nucleophilic centers, which governs the strength of bonds, the strength of nonbonded interactions, and molecular reactivity, which in turn affect the strength of the interactions of the ligand with the receptor protein.

Bhattacharjee and Karle have used the MEP to relate the antimalarial potency of carbinolamine analogs²² and the neurotoxicity of artemisinin analogs.²³ An initial MEPS study on the 41 LpxC inhibitors (Table 1 of the Supporting Information-2 file) showed that the inhibitors were more potent when they possessed a large lateral positive potential region across the side chains at C4 and C5 of the phenyl ring and a negative potential adjacent to the carbonyl oxygen atom of hydroxamic acid and the oxazoline ring. The overall positive potential on the van der Waals surface of the molecules has been observed to be in the range of 26.7–

Table 5. Selected Electronic and Surface Properties and pIC₅₀ Values of Dual PDE4–TNF α Inhibitors Proposed as LpxC Inhibitors

compounds	pIC ₅₀	most negative potential (kcal/mol)	most positive potential (kcal/mol)
L3	6.48	−51.9	34.3
(S)-1b	4.64	−48.3	33.4
2a	4.83	−55.5	43.3
10	5.44	39.7	−48.1
1f	4.69	48.2	−56.9
(S)-1a	4.79	−48.1	47.1
(R)-2b	5.05	−64.0	57.4
(R)-1b	4.58	−47.0	32.2
6a	4.79	−51.4	52.3
(S)-2c	5.48	−59.7	59.0
15	5.37	−54.8	64.0
1e	5.37	−50.3	48.7

61.4 kcal/mol, and the negative potential was in the range of −35.6 to −60.9 kcal/mol. Less active LpxC inhibitors did not possess some of these attributes.

A MEP study of dual PDE4–TNF α inhibitors proposed as LpxC inhibitors showed that all of these structurally diverse compounds share specific electronic properties and should be more potent than L3 (Table 5). The overall positive potential on the van der Waals surface of the molecules has been observed to be in the range of 32.2–64.0 kcal/mol, and the negative potential of was in the range of −47.0 to −64.0 kcal/mol. The more negative potential of −50.3 to −64.0 kcal/mol is expressed by the phenoxy oxygen, aromatic nitrogen atom, and carbonyl oxygen atom. The site for the most positive potential ranging from 48.7–64.0 kcal/mol is due the pentenoxy moiety hydroxyl hydrogen. Compound 15 is an exception in which the site for the most negative potential belongs to the carboxyl oxygen atom. These compounds also show a more positive potential near the C-4 and C-5 positions of the phenyl ring due to the presence of the pentenoxy moiety, which is in accordance with the SAR drawn for the LpxC inhibitory series (Table 1 of the Supporting Information-2 file).

Briefly, these studies show that the dual PDE4–TNF α inhibitors share specific molecular electronic properties with the reported molecules regardless of heterocyclic ring type and thus should be potent LpxC inhibitors. The values of the MEP and the shape and distribution of the isopotential surfaces of all the dual PDE4–TNF α inhibitors in this study are essentially different from those found in the reported 41 molecules but maintain common structural requirements for activity.

To identify the potential druglike compounds from this data set, ADME/T analysis was performed. The data was analyzed on five criteria, rule of five (RO5), absorption level, solubility level, hepatotoxicity, and CYP 2D6 inhibition (Table 6; Supporting Information-2, Table 2). RO5 is in part an indicator of the absorption level and CYP 2D6 inhibition an indicator of hepatotoxicity with some additional features considered in the latter case. The compounds have been predicted to be well-absorbed and low on hepatotoxic potential. Additionally, as the CYP 2D6 inhibitory potential of the molecules is also predicted to be low, the chances of undesirable drug interactions are less. The compounds have been predicted to be poorly soluble, which is not a desirable observation. However, this can be improved by the addition

Table 6. ADME/T Property of Proposed Dual PDE4–TNF α Inhibitors as LpxC Inhibitors

properties	absorption	solubility	hepatotox	Cyp2D6 inhibition	rule of 5 violations
desirable range	<9.6	−4.0 to 0.0	0	0	0
observed range	0.4–2.2	3	0	0	0

of solubilizing groups like OH, CO₂H, and so forth at the hydroxamic acid position in the compounds' structure. Such features can be used to improve the ADME/T profile of the compounds without much altering of the therapeutic profile.

CONCLUSION

In view of a multilayer virtual screening protocol, a screening layer, a prediction layer, and a validation layer have been envisaged. In the present study, the focus was primarily on the implementation of a multilayer screening protocol consisting of a descriptor-based QSAR model as a preliminary screening layer, docking, MEPS, and an ADME/T-based filter as a validation layer for the evaluation of *Pseudomonas aeruginosa* deacetylase LpxC inhibitory activity of dual PDE4–TNF α inhibitors. The compounds have shown promising results in in silico testing and can prove to be potential leads for the design of potent LpxC inhibitors.

ABBREVIATIONS

LpxC = UDP-3-*O*-[R-3-hydroxymyristoyl]-GlcNAc deacetylase; PDE4 = phosphodiesterase 4; TNF α = tissue necrosis factor α ; MEPS = molecular electrostatic potentials surfaces; ADME/T = absorption, distribution, metabolism, excretion, and toxicity.

Supporting Information Available: Additional detailed results are described in Supporting Information-1, -2, and -3. This material is available free of charge via the Internet at <http://pubs.acs.org>.

REFERENCES AND NOTES

- Jacobsson, M.; Liden, P.; Stjernschantz, E.; Bostrom, H.; Norinder, U. Improving Structure-Based Virtual Screening By Multivariate Analysis of Scoring Data. *J. Med. Chem.* **2003**, *46*, 5781–5789.
- So, S. S.; Karplus, M. Evaluation of Designed Ligands by a Multiple Screening Method: Application to Glycogen Phosphorylase Inhibitors Constructed With a Variety of Approaches. *J. Comput.-Aided Mol. Des.* **2001**, *15*, 613–647.
- Prathipati, P.; Saxena, A. K. Evaluation of Binary QSAR Models Derived From Ludi and Moe Scoring Functions For Structure-Based Virtual Screening. *J. Chem. Inf. Model.* **2006**, *46*, 39–51.
- Pirrung, M. C.; Tumey, L. N.; McClerren, A. L.; Raetz, C. R. H. High-Throughput Catch-and-Release Synthesis of Oxazoline Hydroxamates. Structure-Activity Relationships in Novel Inhibitors of *Escherichia coli* LpxC: In Vitro Enzyme Inhibition and Antibacterial Properties. *J. Am. Chem. Soc.* **2003**, *125*, 1575–1586.
- Kleinman, E. F.; Campbell, E.; Giordano, L. A.; Cohan, V. L.; Jenkinson, T. H.; Cheng, J. B.; Shirley, J. T.; Pettipher, E. R.; Salter, E. D.; Hibbs, T. A.; DiCapua, F. M.; Bordner, J. Striking Effect of Hydroxamic Acid Substitution on The Phosphodiesterase Type 4 (PDE4) And TNF Alpha Inhibitory Activity of Two Series of Rolipram Analogues: Implications For A New Active Site Model of PDE4. *J. Med. Chem.* **1998**, *41*, 266–270.
- Kline, T.; Andersen, N. H.; Harwood, E. A.; Bowman, J.; Malanda, A.; Endsley, S.; Erwin, A. L.; Doyle, M.; Fong, S.; Harris, A. L.; Mendelsohn, B.; Mdluli, K.; Raetz, C. R.; Stover, C. K.; Witte, P. R.; Yabannavar, A.; Zhu, S. Potent, Novel In Vitro Inhibitors of the *Pseudomonas aeruginosa* Deacetylase LpxC. *J. Med. Chem.* **2002**, *45*, 3112–3129.
- SYBYL, version 7.1; Tripos Inc.: St. Louis, MO, 2005.

- (8) Dewar, M. J. S.; Zebisch, E. G.; Healy, E. F.; Stewart, J. J. P. Development and Use of Quantum Mechanical Molecular Models. 76. AM1: A New General Purpose Quantum Mechanical Molecular Model. *J. Am. Chem. Soc.* **1985**, *107*, 3902–3909.
- (9) Mulliken, R. S. Electronic Population Analysis on LCAO-MO Molecular Wave Function I. *J. Chem. Phys.* **1955**, *23*, 1833–1846.
- (10) Dragon, version 5; Milano Chemometrics and QSAR Research Groups Inc.: Italy, 2004.
- (11) Hasegawa, K. M.; Funatsu, Y. GA Strategy for Variable Selection in QSAR Studies: GA-Based PLS Analysis of Calcium Channel Antagonists. *J. Chem. Inf. Comput. Sci.* **1997**, *37*, 306–310.
- (12) Rogers, D.; Hopfinger, A. J. Application of Genetic Function Approximation to Quantitative Structure–Activity Relationships and Quantitative Structure–Property Relationships. *J. Chem. Inf. Comput. Sci.* **1994**, *34*, 854–866.
- (13) Hahn, M. R. Receptor Surface Models: 2. Application to Quantitative Structure–Activity Relationships Studies. *J. Med. Chem.* **1995**, *38*, 2091–2102.
- (14) Tokarski, S. H. Constructing Protein Models for Ligand–Receptor Binding Thermodynamic Simulations: An Application to a Set of Peptidomimetic Renin Inhibitors. *J. Chem. Inf. Comput. Sci.* **1997**, *37*, 779–791.
- (15) Tokarski, S. H. Prediction of Ligand–Receptor Binding Thermodynamics by Free Energy Force Field (FEFF) 3D-QSAR Analysis: Application to a Set of Peptidomimetic Renin Inhibitors. *J. Chem. Inf. Comput. Sci.* **1997**, *37*, 792–811.
- (16) Shi, L. M.; Yi, F.; Myers, T. G.; O'Connor, P. M.; Paull, K. D.; Friend, S. H. Mining The NCI Anticancer Drug Discovery Databases: Genetic Function Approximation For The QSAR Study Of Anticancer Ellipticine Analogues. *J. Chem. Inf. Comput. Sci.* **1998**, *38*, 189–199.
- (17) Venkatarangan, P.; Hopfinger, A. J. Prediction of Ligand–Receptor Binding Thermodynamics by Free Energy Force Field Three-Dimensional Quantitative Structure–Activity Relationship Analysis: Applications to a Set of Glucose Analogue Inhibitors of Glycogen Phosphorylase. *J. Med. Chem.* **1999**, *42*, 2169–2179.
- (18) Gokhale, V. M.; Kulkarni, V. M. Understanding the Antifungal Activity of Terbinafine Analogues Using Quantitative Structure–Activity Relationship (QSAR) Models. *Bioorg. Med. Chem.* **2000**, *8*, 2487–2493.
- (19) Cerius², version 4.10; Accelrys Inc.: San Diego, CA, 2005.
- (20) Whittington, D. A.; Rusche, K. M.; Shin, H.; Fierke, C. A.; Christianson, D. W. Crystal Structure Of LpxC, a Zinc-Dependent Deacetylase Essential for Endotoxin Biosynthesis. *Proc. Natl. Acad. Sci. U.S.A.* **2003**, *100*, 8146–8150.
- (21) Clure, C. P.; Rusche, K. M.; Peariso, K.; Jackman, J.; Fierke, C. A.; Penner-Hahn, J. E. EXAFS Studies of the Zinc Sites of UDP-(3-O-Acyl)-N-Acetylglucosamine Deacetylase (LpxC). *J. Inorg. Biochem.* **2003**, *94*, 78–85.
- (22) Bhattacharjee, A. K.; Karle, J. M. Functional Correlation of Molecular Electronic Properties with Potency of Synthetic Carbinoamines Antimalarial Agents. *Bioorg. Med. Chem.* **1998**, *6*, 1927–1933.
- (23) Bhattacharjee, A. K.; Karle, J. M. Stereoelectronic Properties of Antimalarial Artemisinin Analogues In Relation To Neurotoxicity. *Chem. Res. Toxicol.* **1999**, *12*, 422–428.

CI600364B